Article

The Decoherence of the Electron Spin and Meta-Stability of ^{13}C Nuclear Spins in Diamond

Peter Crompton

School of Mathematics, University of East Anglia, Norwich, NR4 7TJ, UK;

E-Mail: peter.crompton@uea.ac.uk; Tel.: +44-(0)-1603-592868; Fax: +44-(0)-1603-593868.

Abstract: Following the recent successful experimental manipulation of entangled ^{13}C atoms on the surface of Diamond, we calculate the decoherence of the electron spin in Nitrogen Vacancy NV centers of Diamond via a nonperturbative treatment of the time-dependent Greens function of a Central-Spin model in order to identify the Replica Symmetry Breaking mechanism associated with intersystem mixing between the $m_s = 0$ sublevel of the $^3A_2$ and $^1A_1$ states of the NV^- centers, which we identify as mediated via the meta-stability of ^{13}C nuclei bath processes in our calculations. Rather than the standard exciton-based calculation scheme used for quantum dots, we argue that a new scheme is needed to formally treat the Replica Symmetry Breaking of the $^3A_2 \to {}^3E$ excitations of the NV^- centers, which we define by extending the existing Generalized Master Equation formalism via the use of fractional time derivatives. Our calculations allow us to accurately quantify the dangerously irrelevant scaling associated with the Replica Symmetry Breaking and provide an explanation for the experimentally observed room temperature stability of Diamond for Quantum Computing applications.

Keywords: topological mixing; replica symmetry breaking; entanglement; quantum computing; CP violation

1. Introduction

Recently, several experimental groups [1–4] have investigated the feasibility of processing Quantum Information via the manipulation of optically excited electron spins [5] in Diamond, with a focus on

Diamonds' optically active Nitrogen Vacancy (NV) centers. These NV centers are formed by the substitutional change of a Carbon for a Nitrogen atom in the Diamond lattice, which can create a lattice vacancy, and optical experiments have indicated that these point defects have trigonal symmetry C_{3v}, where the C_3-axis is the crystallographic [111]-direction of the NV center [6]. Explicitly, this point symmetry group C_{3v} is defined as the group of rotations of a 3-sided pyramid in 3-dimensions about a point which leaves the origin invariant, and consequently, C_{3v} is a subgroup of the rotation group of 3-dimensional space $SO(3)$ [7]. In this article we essentially argue that this has important consequences when we come to define qubits via the NV centers using standard association of the qubit with the S_z eigenvectors of a spin state represented via $SU(2) \simeq SO(3)/\mathbb{Z}_2$, which have not been discussed elsewhere. A simple way is to picture the allowed group operations of C_{3v} as the possible reflections of the vertices of 3-sided pyramid which sits inside a sphere (where all vertices touch the surface). Assigning the integers $1, 2$ and 3 to the vertices of the 3-sided pyramid (opposite to the fixed origin) the Young tableaux [7] for the irreducible representations of the allowed states in C_{3v} are

$$A_1 \equiv \boxed{1\,2\,3}\,, \quad E \equiv \begin{array}{|c|c|}\hline 1 & 2 \\\hline 3 \\\cline{1-1}\end{array} \text{ or } \begin{array}{|c|c|}\hline 1 & 3 \\\hline 2 \\\cline{1-1}\end{array}\,, \quad A_2 \equiv \begin{array}{|c|}\hline 1 \\\hline 2 \\\hline 3 \\\hline\end{array} \tag{1}$$

note that the state E can be antisymmetrized in two possible ways (with respect to 2 or 3), whereas the state A_1 is totally symmetric, and the state A_2 is totally antisymmetric under the C_{3v} symmetry operations, where in the above notation rows symmetrize whilst columns antisymmetrize [7]. There are two known charged states of the NV point defect, which are the neutral and negatively charged NV^0 and NV^- centers [8,9], although the term NV center is usually taken to refer just to the NV^- center. Applying a magnetic field along one of the four equivalent [111]-directions leaves three of the C_{3v} subgroups of an NV center magnetically degenerate, implying that the optically excited electrons come from a triplet state [6]. However, it was not initially clear whether the measured optical (Electron Paramagnetic Resonance) signals for Diamond corresponded to the transition $^1A_1 \rightarrow {}^3A_2 \rightarrow {}^1E$ or $^3A_2 \rightarrow {}^3E$, although this is now settled, with $^3A_2$ understood as the electron spin triplet ground state of the NV^- center [6,10]. This NV^- center ground state consists of six electrons (an additional one having been acquired from the lattice) and the $m_s = 0$ level has a zero-field splitting of $D = 2.88\,GHz$ into a singlet and doublet [11]. A more detailed picture of the experimental difficulties associated with the identification of the nature of the ground state transitions of the two NV charged states are given in [12–14].

In the above experimental studies [1–4] the proposal has been to form qubits consisting of a single electron spin in the NV^- center by optically exciting the $^3A_2$ state [12]. This state then slowly decoheres via the spectral diffusion of the nuclear spin polarizations of the neighboring nuclear spins which are coupled to the single electron in the absence of optical excitation (for example, by the flip-flop transitions of the nuclear spins [15]). Diamond offers several advantages over conventional Quantum Dot materials, such as GaAs for this purpose [11,16], because the density of states is relatively low (with a low electron-phonon coupling), whilst the oscillator strength for the electron dipole transition is relatively large (*i.e.*, Diamond is hard and optically active) [10,17]. These properties of Diamonds NV centers are true in particular for the electron's coupling to the ^{13}C atoms which have a natural abundance of 1.1% [2]. Consequently, it has been reported that (inhomogeneous) electron spin-dephasing times of

$T_2^* = 0.5 - 6\ \mu$s can be achieved in Diamond, at 300 K-without the need for cryogenic cooling [1,4,18], which makes Diamond an attractive candidate for Quantum Information Processing. Following [12], however, we argue that whilst it is clear that a successful qubit can be constructed from the spin polarization the $^3A_2$ state (as has been successfully demonstrated in [1,4,9,16,17]) it is not at all clear why this state should be so highly stable from a calculational standpoint, with such a relatively long decoherence time, given the current understanding of the mechanism of spectral diffusion [19,20].

The intersystem crossings of the excitations of the $^3A_2$ ground state of NV^- are slightly unusual [12], and are essentially the subject of our discussion. For the NV^- state, measurements indicate that the linearly polarized optical excitation of the $^3A_2 \rightarrow {}^3E$ transition and the average photon emission rate are strongly enhanced for the $m_s = 0$ over the $m_s = \pm 1$ levels, which has been attributed to a crossing to the singlet $^1A_1$ level and intersystem mixing [21]. Furthermore, optical measurements with an applied external electric field have shown the disappearance of certain ^3E excitation lines, which has again been attributed to an intersystem mixing [10]. Specifically, in the absence of an applied field it is known that the ^3E splitting is caused by spin-spin or axial $\lambda L_z S_z$ spin-orbit interaction but that this cannot cause an S_z and $S_{x,y}$ mixing, whereas with an applied electric field orthogonal to z the ^3E sublevels can split and mix as $\pm (F_x^2 + F_y^2)^{1/2}$, where F is the applied field strength [10]. Therefore the spin-orbit coupling of the central electrons in the NV^- centers may be sufficient to induce an intersystem crossing to states with a different spin symmetry, *i.e.*, the singlet state [22]. The unusual aspect of this is that if (as calculated in the [12]) the ^1E singlet excitation of NV^- in fact lies below the $^1A_1$ singlet level, then this spin polarization should occur in the $S_{x,y}$ direction rather than S_z.

Intuitively, the two excitons corresponding to the excitations of the ground state of the NV^0 center ($^2E \rightarrow {}^2A_1$ [23]) and NV^- center ($^3A_2 \rightarrow {}^1A_1(^1E) \rightarrow {}^3E$) are not formally related: they correspond to two different representations of the same fundamental group C_{3v} [24], and are therefore physically different systems (not least of all because they correspond to systems with different electric charges). In one case the NV center has five electrons, whilst in the other the NV center has picked up an itinerant electron from the lattice and has 6 electrons, and so intuitively the dynamics of the NV^0 center and NV^- center are uncoupled. However, it is our argument in this article that it is not the case. Physically, we argue that the theory which explains the experimentally observed pattern of intersystem mixing of the excitations of $^3A_2$ (and subsequent decoherence of spin polarization) involves including the source of the itinerant electron which gives rise to the triplet $^3A_2$: We make this distinction in order to fully define the system that the proposed qubit [12] is entangled with. Mathematically, the common sense intuition for why these two ground states (the NV^0 center doublet ^2E, and NV^- center triplet $^3A_2$) are unrelated can be expressed formally by saying that, within the path integral for a multiply connected space, paths in different homotopy classes cannot be continuously deformed into each other. However, the mathematical subtlety that defies this common sense intuition arises from noticing that although such paths cannot be deformed into each other, they can have the same weight in the path integral of the multiply connected space and, moreover, these weights form a one-dimensional unitary representation of the fundamental group of the space [25]. Physically, we intuitively understand that this means that when a proposed qubit decoheres it does not do so to a unique state of the system, but rather to a continuum of degenerate states, and we say that the qubit state has obtained some entanglement phase angle θ, where qubit representation $|\phi\rangle \rightarrow e^{i\theta}|\phi\rangle$. To be clear, the actual mechanism of decoherence of the single electron spin that we

consider in this article is the conventional spectral diffusion that has been considered previously [15], which occurs in the absence of optical excitation of the $^3A_2$ state and therefore preserves the parity of the qubit. However, it is our new argument that this qubit does not simply decohere to become entangled with the bath, but with a bath which is also decohering to become entangled with itself and, therefore, that this slowly changes the definition of the $SO(3)$ rotational symmetry of the electron spin to make it evolve into an oblate spheroid (relative to its initial spin projection). Whilst previous calculational schemes have treated the nuclear spin bath dynamics [19,20], these schemes have been restricted to short-time regimes and localised electron states, which we are now able to go beyond in our new approach. The limitation we have resolved is that there is generally a two-scale process involved in bath dynamics: The range of the nuclear dipole interaction strength and the cluster size of the frozen cores of nuclear spins that form through the flip-flop processes [19], and it was not previously understood to be possible to define a expansion program that is simultaneously valid at two very different scales. However, we have now used topology to define geodesics for the system such that there are no expansion parameters: Rather the two charged states of Diamond are separated via an exact branch point in the time evolution of the system. Hence, the new mechanism we consider in this article for Diamond does not itself drive the spin decoherence of the qubit, but rather it rescales the time-dependence via the time-evolving decoherence of the bath which, we argue, accounts for the relatively long decoherence time of the qubits formed in Diamond.

Conventionally, calculating the tensor product of any two irreducible representation allows us to accurately determine which are the allowed transitions of, either, the $^2E \rightarrow {}^2A_1$ exciton of the NV^0 center, or (completely independently), the $^3A_2 \rightarrow {}^1A_1(^1E) \rightarrow {}^3E$ exciton of the NV^- center, on the basis of whether the resulting tensor product contains as a subgroup the totally symmetric irreducible representation of C_{3v}. Similarly, if the resulting tensor product contains as a subgroup the electric dipole moment, this allows us to determine which transitions are optically allowed (the $^3A_2 \rightarrow {}^1A_1(^1E) \rightarrow {}^3E$ transitions are therefore not), and following similar reasoning, the conventional explanation for the zero mode splitting of the NV^- center is that it arises from the spin-spin dipole interaction (to a first order approximation) since this is the simplest parity-preserving self-interaction that involves the triplet [26]. To see explicitly how this argument is modified for our discussion we consider three (degenerate) qubit spin-1/2 states that are defined via S_z eigenvectors of a spin state represented via $SU(2) \simeq SO(3)/\mathbb{Z}_2$, and place each on the vertices of the 3-sided pyramid defined for the irreducible representations of the allowed states in C_{3v}

$$\boxed{1} \otimes \boxed{2} \otimes \boxed{3} = \left(\begin{array}{c} \boxed{\begin{array}{c}1\\2\\3\end{array}} \end{array} \right) \oplus \boxed{\begin{array}{cc}1&2\\3\end{array}} \oplus \boxed{\begin{array}{cc}1&3\\2\end{array}} \oplus \boxed{\begin{array}{ccc}1&2&3\end{array}} \tag{2}$$

and as we would expect this reproduces the picture for the allowed states for the ground state doublet ^2E (as constructed from parity symmetric qubits). However, if we generalize the definition of the qubits so that they are defined via $PSL_2(\mathbb{R})$ (the fundamental group of linear transformations between spin-1/2 states defined on $\mathbb{C}^2$-an oblate spheroid generalization of the spherically symmetric case) the triplet state in brackets is then also allowed [27,28]. To compare the NV^0 and NV^- projection onto the spin-1/2 qubit states, we can define the relationship between the irreducible representations of both

states (denoted $\prod_{\sigma_j}$ for NV^0, and $\prod_{\sigma'_j}$ for NV^-) via the fusion algebra (Littlewood-Richardson) coefficients [25,28]

$$\prod_{\sigma_j} \otimes \prod_{\sigma_k} = \bigoplus_{\sigma'_j} \lambda^{\sigma'_j}_{\sigma_j S_k} \prod_{\sigma'_j} \tag{3}$$

where j is the total number of NV centers being considered as defining the system. For the simplest (qubit parity symmetric) case with $j = k$, the above identity corresponds to the defining relation between the fundamental and adjoint representations of $SU(2)$, with $\mathbf{2} \otimes \mathbf{2} = \mathbf{1} \oplus \mathbf{3}$ and the coefficients are the familiar Clebsch-Gordon coefficients. However, if we generalize the qubit definition so that they are not parity symmetric with ($j \neq k$) we can still generate the same fusion coefficients if we define there to be a $\mathbb{Z}_2$ symmetry describing the electric charge conjugation operation C for the two representations j and k (which are slightly different ellipses). Physically, our argument is that the itinerant electron has already entangled with the system by having been dragged across the lattice in a non-ergodic way (losing energy via the dissipative process we consider in this article) in such a way that the proposed qubit defined via $^3A_2$ should be really identified initially as $e^{-i\theta}|\phi\rangle$. Indeed, such a vibronic coupling picture was one of the initial motivations for the introduction of the Berry phase θ to discuss the Jahn-Teller effect [24]. Our argument is that it is a mechanism of CP (charge–parity) violation that gives rise to the entanglement phase angle θ and zero-field splitting of the $^3A_2$ state. The CP violation is rarely mentioned outside High Energy Physics because it is known that the coupling constants involved in defining this process for the electromagnetic interaction have to be strong (although in principle the mechanism is only a second order electromagnetic effect) [29]. However, our argument is that the itinerant electron that allows the formation of the $^3A_2$ ground state is not a fundamental particle, but rather the concatenation of a series of dissipative processes across the lattice, which makes it strongly coupled [30]. This modifies the conventional argument used to describe the zero-mode splitting of the NV^- center [26] by identifying that if the single electron spins in Diamond are effectively made more oblate as function of time, via the dissipative processes of the bath, then higher order spin-spin moments (quadropole, octopole *etc.*) can rescale to become degenerate with the spin-spin dipole interaction, which provides a competing (and degenerate) mechanism for generating the zero-field splitting. Therefore, whilst conventionally the $^3A_2 \rightarrow {}^1A_1({}^1E) \rightarrow {}^3E$ transitions are optically forbidden (and the spin decoherence mechanism of the $^3A_2$ qubit occurs in the dark [1–4]), in our new approach we say that the small probability that this tunneling occurs in the dark is greatly enhanced because time is effectively rescaled via the degeneracy of the mechanism for generating the zero-field splitting.

The basic differential conductance transport calculation that is important for building a Quantum Computing device using these NV centers Diamond (and manipulating these centers via electrical currents) is the decoherence of the single electron spin associated with the NV center [20]. As shown above, at least in principle, this NV center can then be manipulated as a qubit for Quantum Information processing [1–4]. We argue, however, that the calculation of this decoherence mechanism for the special case of Diamond shares stronger parallels with the determination of the Replica Symmetry Breaking mechanisms of other models of Statistical Mechanics, such as Sherrington-Kirkpatrick spin-glasses [31]. Namely, that in broad terms, we are interested in determining the expectation of the NV^- center spin

S which is interacting with a number of ^{13}C nuclear spins defined through the general spin operators of the Hamiltonian

$$H^{(n)} = \sum_{a=1}^{n} H_J(\{\sigma(a)\}), \quad H_J = \sum_{i,k} \sigma_i J_{i,k} \sigma_j - \sum_i h_i \sigma_i \tag{4}$$

with n the number of replicas of the same spin configuration, via the general interaction couplings $J_{i,k}$, but which is also subject to averaging of the two different possible charged states of the NV centers $(a = 1, 2)$

$$\overline{\langle S \rangle} = \frac{1}{n!} \sum_{\prod} S(q_{\prod(a),\prod(b)}), \quad q_{a,b} = \frac{1}{N} \sum_i \sigma_i^a \sigma_i^b \tag{5}$$

The additional level of complexity that this introduces is that the system can then exist in a regime in which the above θ-replica symmetry that we have identified is broken, but the additional ultrametricity condition which bounds the expectation of both sides of (3) is not satisfied [31], so there is an additional scaling behavior which we quantify in this article. This is the scaling regime where, for example, the charge conjugation symmetry C is broken but the parity symmetry P is not, which is the physical theory that is relevant for describing the qubit defined by the spin polarization of the $^3A_2$ triplet state but which, we argue, cannot be identified directly. The relevant type of disorder in this new mechanism is bond disorder, but our argument is that it only applies within a convex hull of the space of random-field disordered states, because of the dissipative dynamics of spin polarization decoherence.

In this article we consider the dynamics of the model whereby the two ground states of the NV center—the ^2E doublet and $^3A_2$ triplet—are topologically coupled via a replica symmetry defined via the fusion coefficients in (3). This article forms a continuation of the argument we developed in [32,33], where we proposed that the ultrametricity regime of replica symmetry breaking models is the most applicable method for modeling quantum memory. In this article we probe the same basic mechanism via a GME approach for Diamond, but use the relatively new approach of using fractional time derivatives to introduce topological mixing (replica symmetry breaking) into a standard formalism, rather than compute the convexity of the hull of the eigenvalue spectra explicitly as we did in [32,33]. Physically, whilst our qubit basis $|0\rangle$ is (conventionally) defined with respect to the NV^- center triplet ground state $^3A_2$, our qubit basis state $|1\rangle$ requires detailed knowledge of the dissipative processes involved in moving the itinerant electron around the lattice system, which accurately reflects the experimental picture of the intersystem mixing between the $m_s = 0$ sublevel of the $^3A_2$ and $^1A_1(^1E)$ states of the NV^- centers. It is important to note that, although we are considering an operator-product expansion of topological mixing between two ground states with different electric charges, the itinerant electron which creates these different ground states is neither spontaneously created nor destroyed in this process—it remains part of the complete system (associated with another NV center when not forming the local NV^- state), and we merely shift its location across a globally neutrally charged system to locally create either the triplet or doublet ground state of the NV center.

2. Central-Spin Model

Experimentally, there is some evidence that intersystem mixing is important for understanding NV centers in Diamond [6,21,22]. However, the reason why the identity in (3) is important for calculations

of the spin decoherence of a single electron spin in Diamond is that the general three point correlator of a Dirac particle (such as an electron) scales as [34]

$$\langle \overline{\psi}_1(0)\psi_1(0)\overline{\psi}_2(t)\psi_2(t)\overline{\psi}_3(t')\psi_3(t') \rangle = |t|^d \, |t-t'|^d \tag{6}$$

where $0 < t < t'$ is the location of each particle and d is the scaling dimension. Furthermore, this three point correlation function is only analytic for $t \neq t'$, and it is not possible to interchange t, t' without encountering some singularity when these two points collide (formally, this is known as dangerously irrelevant scaling [34]). However, from (3), because we are including intersystem mixing simple time dependent correlators $\langle \boldsymbol{S}^-(0)\boldsymbol{S}^+(t) \rangle$ will actually be of the form of (6) and, therefore, may be singular at some undetermined additional point t'. To be clear, the experimental proposal for making qubits from Diamond in [1–4] is to form a qubit via a single spin in the NV^- center coupled to a bath of the neighboring ^{13}C nuclear spins, which slowly decoheres via the spectral diffusion of the nuclear spin polarizations (for example, by the flip-flop transitions of the nuclear spins [15]). However, here we are proposing a new and different mechanism for the spin decoherence of this system which has not appeared elsewhere in the experimental or theoretical (exciton) literature. Namely, that if intersystem mixing is included in this model (between the $m_s = 0$ sublevel of $^3A_2$ and $^1A_1$), then the spectral diffusion of the bath nuclei (by, flip-flop processes other internuclei interactions) can potentially become dangerously irrelevant.

Our model is defined by the Hamiltonian for a single electron spin in the $^3A_2$ state of the NV^- center of Diamond interacting via: the spin coupling of the electron, the spin coupling of the ^{13}C nuclei, the Hyperfine coupling between the electron and a spin-bath of ^{13}C nuclear spins, and the dipole-dipole interaction between the ^{13}C bath nuclei [19], which is given via the following Central-Spin model Hamiltonian [35–38]

$$H = \epsilon_S B \boldsymbol{S}^z + \sum_{i=1}^{N} \epsilon_I B \boldsymbol{I}_i^z + \sum_{i=1}^{N} A_i \boldsymbol{S} . \boldsymbol{I}_i^z + \sum_{i=1}^{N} \sum_{i \neq j, j=1}^{N} \frac{\epsilon_{dd}}{r_{ij}^3} \left[(\boldsymbol{I}_i . \boldsymbol{n}_{ij}) (\boldsymbol{I}_j . \boldsymbol{n}_{ij}) - \boldsymbol{I}_i . \boldsymbol{I}_j \right] \tag{7}$$

where $\boldsymbol{S}^z$ is the z-component (longitudinal) of the electron spin in the triplet of the $^3A_2$ state (with the z-axis oriented in the [111]-direction of the NV center), $\boldsymbol{I}_i^z$ is the z-component (longitudinal) of the spin of the ith ^{13}C nucleus in the spin-bath, $\boldsymbol{S}$ is the electron spin in the singlet of the $^3A_2$ state, $\boldsymbol{I}_i$ is the spin of the ith ^{13}C nucleus in the spin-bath, N is the number of bath nuclei and $\boldsymbol{n}_{ij}$ is a unit vector linking the centers of the ith and jth ^{13}C nuclear dipole moments with separation r_{ij}. The remaining constants defining the relative strength of the couplings of the Zeeman, Hyperfine and dipole-dipole interactions in Diamond and are given by $\epsilon_S = 115.6 \, \mu eVT^{-1}, \epsilon_I = 0.1196 \, \mu eVT^{-1}, A_i = 0.09873 \, \mu eV$, and $\epsilon_{dd} = 1.2566 \times 10^{-4} \, \mu eV$ [36]. We choose the $\boldsymbol{n}_{ij}$ such that the centers of the ^{13}C nuclear dipole moments are simply arranged in a line, in the plane of the applied external magnetic field (the longitudinal/z-direction), which allows us to model the applied external electric field results in [6] as well as the singlet $^1A_1$ level and intersystem mixing in [21]. It is important to note that there is a hidden zero-field splitting term in (7) given via our new approach (which otherwise uses a conventional formalism). Namely, that since we are considering a rescaling of the oblateness of the $\boldsymbol{S}$ spin operators, via (6), this generates an explicit gap between the $^3A_2$ and E_2 states, via the fusion coefficients in (3). However, rather than explicitly calculating this term in what follows, we will continuously rescale this

contribution back into the dynamics in our new determination of the decoherence time of the $^3A_2$ qubit in Diamond, such that the oblate deformation then defines a geodesic across the multiply defined space that spans the NV^- and NV^0 representations given in (3), and the transformation $|\phi\rangle \rightarrow e^{i\theta}|\phi\rangle$ generates an explicitly parity invariant qubit to match with the state measured in the experimental proposal in [1–4].

3. The Generalized Master Equation

Unfortunately, by including a dipole-dipole interaction in (7) in addition to the Hyperfine interaction, it is not possible to solve this system exactly, since the Hamiltonian in (7) can only be expressed in Jordan-normal form (and not fully diagonalized) [19,36]. However, it is possible to treat the intersystem mixing model in (3) via the General Master Equation prescription in [20] by making the simple, yet rigorous, step of changing time from being a linear to a nonlinear variable $t \rightarrow t^\nu$.

Via Sturm-Liouville theory (in the absence of the dipole-dipole interaction), the longitudinal and transverse spin components of a single electron in the Central-Spin model are exactly separable, which yields the following Nakajima-Zwanzig generalized master equations (GMEs) [20]

$$\langle \dot{\boldsymbol{S}}^z\rangle_t = N_z(t) - i\int_0^t dt'\, \Sigma_{zz}(t-t')\langle \boldsymbol{S}^z\rangle_{t'} \tag{8}$$

$$\langle \dot{\boldsymbol{S}}^+\rangle_t = i\omega_n\langle \boldsymbol{S}^+\rangle_t - i\int_0^t dt'\, \Sigma_{++}(t-t')\langle \boldsymbol{S}^+\rangle_{t'} \tag{9}$$

where $N_z = i/2t(\Sigma_{\uparrow\uparrow}(t) - \Sigma_{\downarrow\downarrow}(t))$, Σ_{zz} and Σ_{++} are given by matrix elements of the reduced self energy $\Sigma(t - t')$, $\omega_n \equiv B(\epsilon_S - \epsilon_I) + h_I$, with h_I as the eigenvalue of the initial angular momentum eigenstates of the bath, and B is the applied field strength. Using these two relations, the time dependence of the single electron spin polarization can then be evaluated via Laplace transform. Importantly, however, the above relations have nonperturbative expansions for $\omega_n/N > 1$ and so the self-energy contributions do not resum and can grow as a function of time. For arbitrary initial polarizations in the high field limit, however, the above self-energies can be re-parameterized as continuous functions of the Hyperfine couplings (via $A_k \rightarrow x$) and in the Born approximation (with $\Sigma_{zz} = \Sigma_{zz}^{(2)}(I_\pm(s))$) this yields the functions

$$I_\pm(s) = \frac{1}{4N}\sum_k \frac{A_k^2}{s \mp \frac{iA_k}{2}} \quad\rightarrow\quad I_\pm(s) = \frac{d}{m}\int_0^1 dx \frac{x|\ln x|^\nu}{s \mp ix}, \quad \nu = \frac{d}{m} - 1 \tag{10}$$

where s is the Laplace variable, m is the z projection of the nuclear spin, and d the dimension of the system [20]. Hence, for $\nu < 1$ the single electron spin decoherence envelope will be oscillatory and is governed by nuclei close to the central electron (Markovian), whereas for $\nu > 1$, the single electron spin decoherence envelope will be slowly decaying and governed by the nuclei farthest away (non-Markovian).

However, in the intersystem mixing problem we considered in (7), the Markovian and non-Markovian regimes can become interchanged and, therefore, in a renormalization group sense ν is then a dangerously irrelevant scaling parameter [39–41]. To treat this dangerously irrelevant scaling rigorously, we follow the recent approach of using fractional derivatives to treat diffusion problems [42–44], and

replace the definition of the time derivatives of the single electron spin in (8) and (9) by the following generalized (Caputo) fractional time derivative [45,46]

$$D_{0\,*t}^{\nu}\left(\boldsymbol{S}^-(t)\boldsymbol{S}^+(0)\right) = \frac{1}{\Gamma(1-\nu)} \int_0^t dt' \frac{1}{(t-t')^\nu} \frac{\partial}{\partial t'} \left(\boldsymbol{S}^-(t')\boldsymbol{S}^+(0^+)\right) \tag{11}$$

where $\boldsymbol{S}^-(t)$ and $\boldsymbol{S}^+(0)$ are time evolution operators for the single electron spin in (3) at time $t' = 0$ and $t' = t$ [47]. This fractional derivative approach is based on the generalization of the Brownian motion of the paths that are required for Euclidean Feymann path integrals in quantum mechanics to Lévy random processes [44]. Rather than the GME being meromorphically continued into poles in (10), formally, the GME defined through (11) is meromorphically continued onto the annulus corresponding to one-dimensional unitary representation of the fundamental group of the multiply connected space [25]. Practically, evaluating spin correlators in this fractional derivative formalism leads to an overall constant in front the correlators compared to the conventional GME, since the Fourier transform of a fractional derivative is given by [48]

$$\mathcal{F}\left[D_\theta^\nu \left(\boldsymbol{S}^-(t)\boldsymbol{S}^+(0)\right)\right] = -\psi_\nu^\theta(t)\mathcal{F}\left[\boldsymbol{S}^-(t)\boldsymbol{S}^+(0)\right], \quad \psi_\nu^\theta(t) = |t|^\nu e^{i\,\mathrm{sgn}(t)\theta\pi/2} \tag{12}$$

Moreover, this constant $\psi_\nu^\theta(t)$ defines the renormalization scale parameter for the intersystem mixing between the $m_s = 0$ sublevel of $^3A_2$ and $^1A_1$ in the NV centers and, therefore, this new approach formally defines a regularization of electron spin decoherence via a ζ-function prescription [33,43,49] as a generalization of the Laplace transform approach in (10).

4. Discrete Fourier Transform

In the nonperturbative regime, electron spin decoherence can be calculated from (8) and (9) using a range of numerical schemes [50]: exact diagonalization [38,51,52], loop-cluster expansion [19,36] and via discrete Fourier transform. In the following analysis we use a discrete Fourier transform method, since we are able to keep the long-time cutoff fixed in a discrete Fourier Transform via the lattice spacing, which allows us to make an accurate comparison of $|t|^\nu$ for different field strengths and polarizations. The advantage of this approach is about having a proper regularization of the GME in a treatment which also includes a full dipole-dipole interaction and the intersystem mixing of the NV center. To be clear, writing the Hamiltonian in block-diagonal form in the product basis $|\psi\rangle = |S \otimes I_1 \otimes I_2 ... \otimes I_N\rangle$ and treating the off-diagonal Hyperfine-interaction components as a perturbation, we yield an energy-dependent Greens function of the form

$$H = \begin{pmatrix} H_{11} & H_{12} \\ H_{21} & H_{22} \end{pmatrix} \tag{13}$$

$$G(\epsilon) = (\epsilon - H_{11})^{-1} H_{12} (\epsilon - H_{22})^{-1} H_{21} (\epsilon - H_{11})^{-1} \tag{14}$$

The above is not a well-defined problem because $[H, \boldsymbol{S}^z] \neq 0$ if there is intersystem mixing between the $m_s = 0$ sublevel of ^3A and ^1A in the NV centers.

We calculate the decoherence of the transverse electron spin by using a discrete Fourier transform to calculate time-dependent Greens function of the Hamiltonian in (1), for up to a maximum of $N = 8$ nuclei. Although $N = 8$ is an experimentally relevant number for current entanglement

studies [2,3,16], this small bath size can further justified for larger quantum dot systems via the convergence of Chebyshev polynomials [50]. Explicitly, if the state vector of the spin-bath is represented via

$$|\chi\rangle = \sum_{k=1}^{N_B} \alpha_k |\, \beta_1 \beta_2 ... \beta_{N_B-1}\,\rangle, \quad \sum_{k=1}^{N_B} |\alpha_k|^2 = 1 \qquad (15)$$

where β is either 0 or 1 (depending on whether the ith bath nuclei is spin up or spin down), α_k is a random variable, and there are $N_B = 2^N$ bath states, then, since the off-diagonal elements are of the order $2^{-N_B}/\sqrt{N_B}$, agreement with the electron spin polarization to 6% of the value for the full system (of $N \sim 10^6$) can be obtained from sampling clusters of just $N = 8$ nuclei. Furthermore, this limit $(2^{-N_B}/\sqrt{N_B})$ is an exact bound for the random Lévy random processes that form the (canonical) basis of our approach, and this formally sets the accuracy of approximating the electron spin correlators via a system consisting of $N = 8$ nuclei [53]. Furthermore, the values of the Hyperfine interaction couplings in (7) can be randomly picked between $0\,\mu eV$ and $0.09873\,\mu eV$ (as we did for this analysis) without significantly impacting on the accuracy of the spin correlator measurements, *i.e.*, the dominant source of error is the size of the spin bath which yields an error of 6%.

As is discussed in [54], a discrete Fourier transform is essentially a family of unitary operators whose eigenvalues have a multiplicity of 4. Consequently, for the purpose of comparing the efficiency of methods, the slow step which limits the computational speed at which the discrete operations can be processed in this calculation is the resolution of this choice of branch point for the eigenvalues, or more correctly, the pivoting that is required to perform this. In [54] the computational complexity of the discrete Fourier transform is explicitly identified by constructing the Weil representation defined over the finite field $SL_2(\mathbb{F}_p)$ in order to find the prime spectra of the transform. The number of steps required for the calculation is found to be $N \log N$, whereas the asymptotic lower bound on a brute force diagonalization calculation is at best N^2. Hence, the discrete Fourier transform is generically faster than brute force diagonalization.

We obtain the energy-dependent Greens function of the Central spin model for Diamond via an exact inversion of the Hamiltonian in (1) using Gauss-Jordan elimination

$$[G(\varepsilon)]_{i,j} = \left[\, (\varepsilon - H)^{-1}\,\right]_{i,j} \qquad (16)$$

where $G(\varepsilon)$ is then a 2^{2N+2} matrix defined in the product basis $|\psi\rangle = |S \otimes I_1 \otimes I_2... \otimes I_N\rangle$. We repeat this calculation for M discrete values of energy, ε, where $G_n(\varepsilon) = G(\varepsilon)|_{\varepsilon=n\Delta\epsilon}$ with $\Delta\varepsilon = E/M$ and E the finite energy domain of the system, which we choose to be of $\mathcal{O}(\epsilon_S)$. The time-dependent Greens function of the Hamiltonian in (3) is then given by the following discrete Fourier transform, $G_k(t) = G(t)|_{t=k\Delta\tau}$, which we evaluated using the numerically efficient Four-Step Fast Fourier Transform [55]

$$G_{k=qP+Q}(t) \;=\; \sum_{r=1}^{p} \left(e^{2\pi i\, rq/p} \left(e^{2\pi i\, rQ/pP} \sum_{R=1}^{P} G_{RP+r}(\varepsilon) e^{2\pi i\, RQ/P} \right) \right) \qquad (17)$$

$$0 < r, q < p, \quad 0 < R, Q < P, \quad pP = M \qquad (18)$$

where $\Delta\tau = T/M$ with T as the finite time domain of the system, and where the short range cutoff is set via $ET = \hbar$ and $M = 2^{14}$, [37]. The time-dependence of the transverse spin of the single electron in the $m_s = 0$ $^3A_2$ state of the NV^- center in Diamond is then given by the expectation

$$\langle \boldsymbol{S}^+ \rangle_t = \langle \psi_0^\dagger\, G^\dagger(t)\, \boldsymbol{S}^z\, G(t)\, \psi_0 \rangle = \Theta(t)\langle \psi_0|\, \boldsymbol{S}^-(t)\boldsymbol{S}^+(0^+)\, |\psi_0\rangle \qquad (19)$$

where the initial single electron state is defined to be $\psi_0 = (\,|0\rangle + |1\rangle\,)\,/\sqrt{2}$, following [19,35,36]. Note that our fractional derivative approach in (12) means that the above expectation for the transverse electron spin is real (and negative) and is also not normalised to unity. This allows us to quantify the nucleation of the ^{13}C bath dynamics via the factor $|t|^\nu$ in (12) corresponding to the renormalization scale dependence of intersystem mixing between the $m_s = 0$ sublevel of $^3A_2$ and $^1A_1$ in the NV centers.

5. Transverse Single Electron Spin Decoherence

We compare our numerical results in the first instance with the perturbative GME results for the Central Spin model with a single electron obtained in [20] for the limits of large applied external magnetic fields and a fully polarized initial system. We expect the behavior of the NV centers of Diamond to be broadly similar in these limits where the intersystem mixing effects are less relevant for Diamond. The zeroth order dynamics result for the transverse single electron spin in (3) is given by

$$\langle \boldsymbol{S}^+ \rangle_t = \langle \boldsymbol{S}^+ \rangle_0 \exp[-t^2/2\tau_c^2 + i(B(\epsilon_S - \epsilon_I) + pN)t] \qquad (20)$$

where p is the fraction of initially polarized states, and τ_c is the transverse electron decoherence time, which from the perturbative expansion of (3) is expected to be relevant to order $2(k + 1)$ when the self-energy is suppressed by a factor of $(\omega_n/N)^k$. From the second term in the exponent in (20), it follows that the decoherence time, τ_c, becomes independent of the applied field strength for large values of field, and that the nonperturbative regime is therefore delineated by $N|B_z| \gg |\frac{A}{g\mu_B}| \sim \mathcal{O}(10\,\mathrm{Gauss})$. Hence, the models we generate consisting of $N = 2 - 6$ nuclear spins will (loosely) be closer to the nonperturbative bound than the models we generate consisting of $N = 8$ nuclear spins.

In Figure 1 we plot our evaluation of the time dependence of the transverse spin component of the single electron state corresponding to the intersystem mixing between the $m_s = 0$ sublevel of $^3A_2$ and $^1A_1$ in the NV centers, $\langle \boldsymbol{S}^+ \rangle_t$, for spin baths of $N = 8$ and $N = 6$ ^{13}C nuclei in Diamond. Clearly, the initial expectation values of the electron spin differ substantially from unity in both Figures. This indicates that the renormalization parameter $\psi_\nu^\theta(t)$ (which normalizes these expectation values to unity via (12)) is small and negative, and that the intersystem mixing is therefore important to the dynamics of the electron spin decoherence in Diamond in these physical regimes, as we would expect from the experimental studies in [6,21,22]. The overall negative sign factor of the expectation values comes from our initial choice of phase for $\psi_\nu^\theta(t)$, where the initial electron state was chosen to be perpendicular to the applied external magnetic field direction oriented along the $[111]-$direction of the NV crystal axis, where $\theta = \pi/2$.

In the left plot of Figure 1 (for $N = 8$ nuclei) the applied external magnetic field is varied between $0 - 100\,\mathrm{Gauss}$, and in the right plot (for $N = 6$ nuclei at $100\,\mathrm{Gauss}$) the angle between the applied field and z-component of electron spin is varied between $\theta = 0 - \pi/2$. The transverse single electron spin decoherence time increases in the left plot from 1 μs to 7 μs as a function of decreasing applied

field strength (although not noticeably so at the scale in Figure 1), and increases in the right plot as a function of increasing θ (polarization) from 2 μs to 6 μs. These trends follow the broad expectations of the zeroth order result in (16): decreasing B prevents the electron from dephasing, whereas increasing the initial polarization increases the dephasing. These results are also consistent with the experimental measurements in [10] where an electric field was applied orthogonally to z, such that the ^3E sublevels split and mixed as $\pm (F_x^2 + F_y^2)^{1/2}$, where F is the applied field strength. Our results are also consistent with the angular dependence of the direction of the applied magnetic field direction that was experimentally measured for this system in [10]. In all Figures our results support the experimental observations reported in [6,21,22], that although the spin-orbit coupling is relatively weak, it is sufficient to induce an intersystem mixing between the singlet states $m_s = 0$ sublevel of $^3A_2$ and $^1A_1$. Physically, this happens because in a small applied field the electron only has a small amount of angular momentum as it precess around the applied field direction. Therefore, the rate of change of angular momentum into the spin bath is a relatively slow process for smaller values of applied field since the change is less energetically favorable. However, electron spins which are initially perpendicular to the nuclear spin bath spins have a greater initial angular momentum projection onto the spin bath, and are therefore less stable and undergo a faster angular momentum exchange.

Figure 1. Time dependence of the transverse component of the single electron spin, $\langle S^+ \rangle_t$, for spin baths of $N = 8$ and $N = 6$ ^{13}C atoms in Diamond. For $N = 8$ the applied field is varied in 0–100 G, whereas for $N = 6$ the applied field direction is varied relative to the z-axis at $100G$. The renormalization scale parameters for these expectations are given via Figure 2.
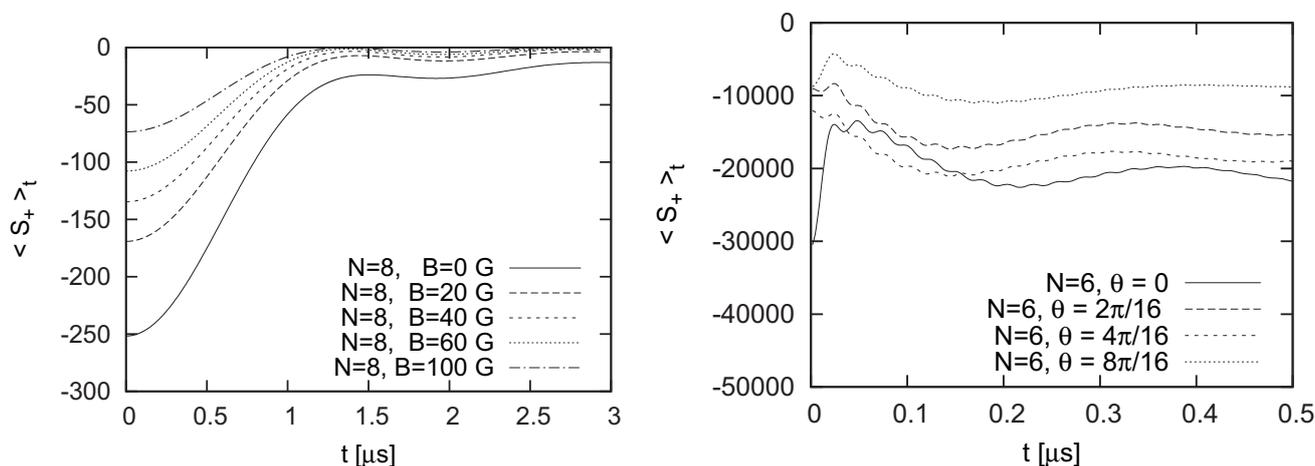
In Figure 2 we plot the applied external magnetic field dependence of the logarithm of expectation value of the transverse single electron spin $\log (\langle S^+ \rangle_T)$. From (12), this gives a measure of the relative differences in the renormalization parameter ν as a function of applied field strength. From Figure 2, evidently the smaller systems (N = 2–6) which are closer to the nonperturbative bound have larger associated values of ν, whereas the larger systems ($N = 8$) which are furthest from the nonperturbative bound have a smaller value of ν. This indicates that the renormalization scale parameter $\psi_\nu^\theta(t)$ is generally larger for smaller systems, and the clear jump in the value of ν between spin baths of size N = 2–6 and $N = 8$ indicates that the intersystem mixing has a different effect on systems in the

Markovian and non-Markovian regimes. Comparing these results for a Replica Symmetry Breaking mechanism for Sherrington-Kirkpatrick spin-glasses [31], we can see that the experimentally effective range of the comparable bond-disorder model would be approximately three times the distance between NV centers. Strictly, however, the relevant type of disorder in this new mechanism is neither bond nor random-field disorder, but rather both, defined within a convex hull set by the random-field disorder through the rescaling via dissipative dynamics mechanism of spin polarization decoherence that we have identified above. Similarly, the decoherence mechanism is strictly neither spin-echo nor free induction decay, but a dynamical combination whereby the spin-echo boundaries (the qubit definition $e^{-i\theta}|0\rangle$, $|1\rangle$) rescale as a function of time. Our results are consistent with the measured experimental decoherence times for isotopically purified samples with very low concentrations of ^{13}C reported in [18] (using our renormalization scale parameter in Figure 2 we obtain $T_2 \sim (0.5\,\mu s)^{1/2} = 2.2\,\text{ms}$), although our argument is that our change in the definition of the qubit will become more important for practical quantum computing applications where the fusion coefficients in (3) become increasingly important. Therefore, although dangerously irrelevant in the renormalization group sense, in the physical regimes we have considered in this study it appears that the intersystem mixing between the $m_s = 0$ sublevel of $^3A_2$ and $^1A_1$ in the NV centers is stablised by an increased number of ^{13}C bath nuclei, and it is tempting to speculate that this is the mechanism which makes Diamond robust enough for Quantum Information Processing at room temperature.

Figure 2. Applied field strength dependence of the logarithm of the argument of the Caputo integral in (13), for spin baths of $N = 2 - 8$ ^{13}C atoms in Diamond.
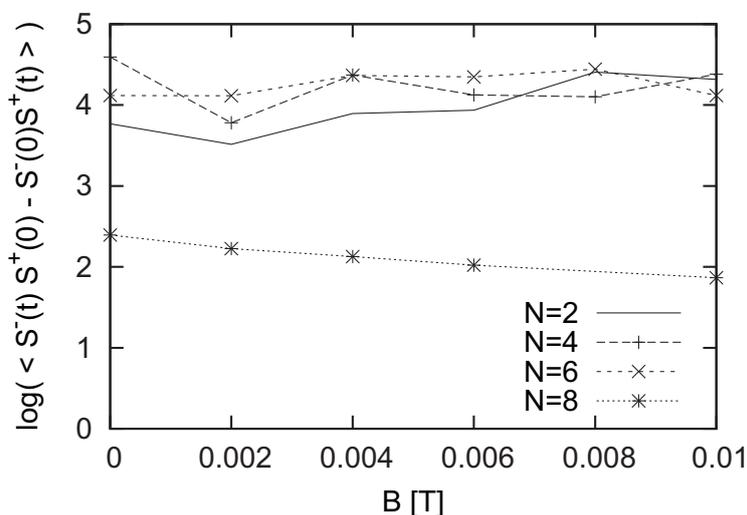
6. Summary

A recent experimental proposal for making qubits from Diamond in [1–4] is to form a qubit via a single electron spin in the NV^- center coupled to a bath of the neighboring ^{13}C nuclear spins, which slowly decoheres via the spectral diffusion of the nuclear spin polarizations (for example, by the flip-flop transitions of the nuclear spins [15]). Here we have proposed a new and different mechanism for the spin decoherence of this system which is not based on the current theoretical (exciton) literature, but rather on the fusion rules for the mixing of the irreducible representations of the C_{3v} which is justified for two dimensional quantum spin systems in [25,56]. This has allowed us to include the experimentally

relevant [6,21,22] intersystem mixing is between the $m_s = 0$ sublevel of $^3A_2$ and $^1A_1$, via the transition $^3A_2 \to {}^1A_1(^1E) \to {}^3E$. We have argued that central to understanding the level ordering of the singlets in this exciton [12] (and their role in the spin relaxation of the qubit formed from the spin polarization of the $^3A_2$ NV^- ground state [1–4]) is a need to clarify the role that the itinerant electron plays in defining the NV^0 and NV^- ground states. In our new approach the irreducible representation of the itinerant electron is noticed to be isomorphic to the qubit on the basis of their respective characterization either via a $\mathbb{Z}_2$ electric charge symmetry or the parity of the qubits. We have solved the dynamics of this system in a way in which both the itinerant electron and qubit are entangled via the same dissipative dynamics mechanism, and argued that this does not imply that we are coupling the dynamics of two different electric charge states, but rather defining a theory in which the itinerant electron is considered to be part of a larger charge neutral system. The $\mathbb{Z}_2$ electric charge symmetry is therefore neither created nor destroyed globally—only locally. We have calculated the transverse electron spin decoherence for the NV^- center in Diamond, modeled as a Central-Spin electron spin coupled to a bath of up to eight entangled ^{13}C nuclei, with an additional dipole-dipole interaction also included between these bath nuclei. Our approach is based on a ζ-function regularization [33] of intersystem mixing between the $m_s = 0$ sublevel of $^3A_2$ and $^1A_1$ in the NV centers, which we have calculated via a fractional time derivative [45–48] generalization of the standard GME approach [20]. Our results for the decoherence time of the transverse electron spin of the NV center are consistent with recent experimental measurements for (proximal) spin baths of this size [1–4,16], and furthermore, our investigation of the regularization of our approach indicates that the stability of the dangerously irrelevant scaling we have identified via our analysis improves as a function of increasing bath size. It is therefore tempting to speculate that the intersystem mixing between the $m_s = 0$ sublevel of $^3A_2$ and $^1A_1$ in the NV centers is the mechanism which makes Diamond robust enough for Quantum Information Processing at room temperature. By treating time as a nonlinear variable we have been able to accurately quantify the metastability of ^{13}C nuclei in the spin bath as they exchange angular momentum with both $m_s = 0$ sublevel of $^3A_2$ and $^1A_1$ in the NV centers, via the renormalization parameter, $\psi_\nu^\theta(t)$.

References

1. Childress, L.; Gurudev Dutt, M.V.; Taylor1, J.M.; Zibrov1, A.S.; Jelezko, F.; Wrachtrup, J.; Hemmer, P.R.; Lukin, M.D. Coherent dynamics of coupled electron and nuclear spin qubits in diamond. *Science* **2006**, *314*, 281–285.

2. Gurudev Dutt1, M.V.; Childress1, L.; Jiang, L.; Togan, E.; Maze, J.; Jelezko, F.; Zibrov, A.S.; Hemmer, P.R.; Lukin, M.D. Quantum register based on individual electronic and nuclear spin qubits in diamond. *Science* **2007**, *316*, 1312–1316.

3. Neumann, P.; Mizuochi, N.; Rempp, F.; Hemmer, P.; Watanabe, H.; Yamasaki, S.; Jacques, V.; Gaebel, T.; Jelezko, F.; Wrachtrup, J. Multipartite entanglement among single spins in diamond. *Science* **2008**, *320*, 1326–1329.

4. Takahashi, S.; Hanson, R.; van Tol, J.; Sherwin, M.S.; Awschalom, D.D. Quenching spin decoherence in diamond through spin bath polarization. *Phys. Rev. Lett.* **2008**, *101*, 047601.

5. Lukin, M.D.; Imamoglu, A. Nonlinear optics and quantum entanglement of ultraslow single photons. *Phys. Rev. Lett.* **2000**, *84*, 1419–1422.

6. He, X.F.; Manson, N.B.; Fisk, P.T.H. Paramagnetic resonance of photoexcited N-V defects in diamond. I. Level anticrossing in the 3A ground state. *Phys. Rev. B* **2001**, *47*, 8809–8815.

7. Cini, M. *Topics and Methods in Condensed Matter Theory: From Basic Quantum Mechanics to the Forefront of Research*; Springer: Berlin, Germany, 2007; pp. 177–178.

8. Felton, S.; Felton, S.; Edmonds, A.M.; Newton, M.E.; Martineau, P.M.; Fisher, D.; Twitchen, D.J. Electron paramagnetic resonance studies of the neutral nitrogen vacancy in diamond. *Phys. Rev. B* **2008**, *77*, 081201(R).

9. Gali, A. Theory of the neutral nitrogen-vacancy center in diamond and its application to the realization of a qubit. *Phys. Rev. B* **2009**, *79*, 235210.

10. Tamarat, Ph. Gaebel1, T.; Rabeau, J.R.; Khan, M.; Greentree, A.D.; Wilson, H.; Hollenberg, L.C.L. Prawer, S.; Hemmer, P.; Jelezko1, F.; *et al*. Stark shift control of single optical centers in diamond. *Phys. Rev. Lett.* **2006**, *97*, 083002.

11. Jelezko, F.; Wrachtrup, J. Single defect centres in diamond: A review. *Phys. Status Solidi A-Appl. Res.* **2006**, *203*, 3207–3225.

12. Delaney, P.; Greer, J.C.; Larsson, J.A. Spin-polarization mechanisms of the Nitrogen-vacancy center in Diamond. *Nano Lett.* **2010**, *10*, 610–614.

13. Manson, N.B.; Harrison, J.P.; Sellars, M.J. The nitrogen-vacancy center in Diamond re-visited. *arXiv* **2006**, arXiv:cond-mat/0601360.

14. Rogers, L.J.; Armstrong, S.; Sellars, M.J.; Manson, N.B. Infrared emission of the NV center in diamond: Zeeman and uniaxial stress studies. *New J. Phys.* **2008**, *10*, 103204.

15. Stoneham, A.M.; Harker, A.H.; Morley, G.W. Could one make a diamond-based quantum computer? *J. Phys. Condens. Matter* **2009**, *21*, 364222.

16. Jelezko, F.; Gaebel, T.; Popa, I.; Domhan, M.; Gruber, A.; Wrachtrup, J. Observation of Coherent oscillation of a single nuclear spin and realization of a two-qubit conditional quantum gate. *Phys. Rev. Lett.* **2004**, *93*, 130501.

17. Wrachtrup, J. Defect center room-temperature quantum processors. *Proc. Nat. Acad. Sci.* **2010**, *107*, 21, 9479–9480.

18. Balasubramanian, J.; Neumann, P.; Twitchen, D; Markham, M.; Kolesov, R.; Mizuochi1, N.; Isoya, J.; Achard, J.; Beck, J.; Tissler, J.; *et al*. Ultralong spin coherence time in isotopically engineered diamond. *Nat. Mater.* **2009**, *8*, 383–387.

19. Witzel, W.M.; Das Sarma, S. Quantum theory for electron spin decoherence induced by nuclear spin dynamics in semiconductor quantum computer architectures: Spectral diffusion of localized electron spins in the nuclear solid-state environment. *Phys. Rev. B* **2006**, *74*, 035322.

20. Coish, W.A.; Loss, D. Hyperfine interaction in a quantum dot: Non-Markovian electron spin dynamics. *Phys. Rev. B* **2004**, *70*, 195340.

21. Epstein, R.J.; Mendoza, F.M.; KatoY.K.; Awschalomv, D.D. Anisotropic interactions of a single spin and dark-spin spectroscopy in diamond. *Nat. Phys.* **2005** *1*, 94–98.

22. Jelezko, F.; Wrachtrup, J. Single defect centers in diamond: A review. *Phys. Status Solidi A-Appl. Res.* **2006**, *203*, 3207–3225.

23. Goss, J.P.; Jones, R.; Breuer, S.J.; Briddon, P.R.; Öberg, S. The Twelve-Line 1.682eV Luminescence Center in Diamond and the Vacancy-Silicon Complex. *Phys. Rev. Lett.* **1996**, *77*, 3041–3044.

24. Davies, G. Dynamic Jahn-Teller distortions at trigonal optical centers in Diamond. *J. Phys. C* **1979**, *12*, 2551–2566.

25. Laidlaw, M.G.G.; DeWitt, C.M. Feyman Functional Integrals for Systems of Indistinguishable Particles. *Phys. Rev. D* **1971**, *3*, 1375–1378.

26. McLachlan, A.D. Spin-spin coupling hamiltonian in spin multiplets. *Mol. Phys.* **1963**, *6*, 441–444.

27. Greiter, M.; Schuricht, D. Many-spinon states and the secret significance of young tableaux. *Phys. Rev. Lett.* **2007**, *98*, 237202.

28. Gómez, C.; Ruiz-Altaba, M.; Sierra, G. *Quantum Groups in Two-Dimensional Physics*; Cambridge University Press: Cambridge, MA, USA, 1996; pp. 300.

29. Bernstein, J. Feinberg, G.; Lee, T.D.; Possible, C,T. Noninvariance in the Electromagnetic Interaction. *Phys. Rev.* **1965**, *139*, 1650–1659.

30. Ham, F.S. Effect of linear Jahn-Teller coupling on paramagnetic resonance in a ^2E state. *Phys. Rev.* **1968**, *166*, 307–321.

31. Marinari, E.; Parisi, G.; Ricci-Tersenghi, F. Ruiz-Lorenzo, J.J.; Zuliani, F. Replica symmetry breaking in short range spin glasses: A review of the theoretical foundations and of the numerical evidence. *J. Stat. Phys.* **2000**, *98*, 973–1019.

32. Crompton, P.R. The quantum noise of ferromagnetic π-Bloch domain walls. *Entropy* **2009**, *11*, 548–559.

33. Crompton, P.R. The partition function zeroes of quantum critical points. *Nucl. Phys. B* **2009** *810*, 542–562.

34. Hastings, M.B.; Sondhi, S.L. Breakdown of conformal invariance at strongly random critical points. *Phys. Rev. B* **2001**, *64*, 094204.

35. Cappellaro, P.; Jiang, L.; Hodges, J.S.; Lukin, M.D. Coherence and control of quantum registers based on electronic spin in a nuclear spin bath. *Phys. Rev. Lett.* **2009**, *102*, 210502.

36. Maze, J.R.; Taylor, J.M.; Lukin, M.D. Electron spin decoherence of single nitrogen-vacancy defects in diamond. *Phys. Rev. B* **2008**, *78*, 094303.

37. Coish, W.A. Loss, D.; Yuzbashyan, E.A.; Altshuler, B.L. Quantum versus classical hyperfine-induced dynamics in a quantum dot. *J. Appl. Phys.* **2007**, *101*, 081715.

38. Bortz, M.; Stolze, J. Exact dynamics in the inhomogeneous central-spin model. *Phys. Rev. B* **2007**, *76*, 014304.

39. Mueller, C.A. Diffusive spin transport. *Lect. Notes Phys.* **2009**, *768*, 277–314.

40. Wang, Z.; Fisher, M.P.A.; Girvin, S.M.; Chalker, J.T. Short-range interactions and scaling near integer quantum Hall transitions. *Phys. Rev. B* **2000**, *61*, 8326–8333.

41. Wang, Z.; Xiong, S. Electron-electron interactions, quantum Coulomb gap, and dynamical scaling near integer quantum Hall transitions. *Phys. Rev. B* **2002**, *65*, 195316.

42. Dong, J.; Xu, M. Applications of continuity and discontinuity of a fractional derivative of the wave functions to fractional quantum mechanics. *J. Math. Phys.* **2008**, *49*, 052105.

43. Lim, S.C.; Teo, L.P. Topological symmetry breaking of self-interacting fractional Klein Gordon field theories on toroidal spacetime. *J. Phys. A Math. Theor.* **2008**, *41*, 145403.

44. Laskin, N. Fractional Schrödinger equation. *Phys. Rev. E* **2002**, *66*, 056108.

45. Naber, M. Time fractional Schrödinger equation. *J. Math. Phys.* **2004**, *45*, 3339.

46. Goychuk, I. Anomalous relaxation and dielectric response. *Phys. Rev. E* **2007**, *76*, 040102(R).

47. Wang, S.J.; Zhao, D.; Luo, H.G.; Cen, L.X.; Jia, C.L. Exact solution to the von Neumann equation of the quantum characteristic function of the two-level Jaynes-Cummings model. *Phys. Rev. A* **2001**, *64*, 052102.

48. Luchko, Y.; Martinez, H.; Trujillo, J.J. Fractional Fourier transform and some of its applications. *Fract. Calc. Appl. Anal.* **2008**, *11*,457–469.

49. Crompton, P.R. Exact nonperturbative renormalization. *Phys. Rev. D* **2006**, *74*, 096001.

50. Zhang, W.; Konstantinidis, N.; Al-Hassanieh, K.A.; Dobrovitski, V.V. Modelling decoherence in quantum spin systems. *J. Phys. Condens. Matter* **2007**, *19*, 083202.

51. Shenvi, N.; de Sousa, R.; Whaley, K.B. Universal scaling of hyperfine-induced electron spin echo decay. *Phys. Rev. B* **2005**, *71*, 224411.

52. de Sousa, R.; Shenvi, N.; Whaley, K.B. Qubit coherence control in a nuclear spin bath. *Phys. Rev. B* **2005**, *72*, 045330.

53. Popescu, S.; Short, A.J.; Winter, A. Entanglement and the foundations of statistical mechanics. *Nat. Phys.* **2006**, *2*, 754–758.

54. Gurevicha, S.; Hadanib, R. On the diagonalization of the discrete Fourier transform. *App. Comp. Harm. Anal.* **2009** *27*, 1, 87–99.

55. Bailey, D.H. FFTs in external or hierarchical memory. *J. Supercomput.* **1990**, *4*, 23–35.

56. Leinaas, J.M.; Myrheim, J. On the theory of identical particles. *Il Nuovo Cimento* **1977**, *37*, 1–23.